

Supporting Information for:

**Considerable Slowdown of Short DNA Fragments Translocation Across a Protein Nanopore  
Using pH-induced Generation of Enthalpic Traps Inside the Permeation Pathway**

Loredana Mereuta<sup>1</sup>, Alina Asandei<sup>2</sup>, Ioan Andricioaei<sup>3</sup>, Jonggwan Park<sup>4</sup>, Yoonkyung Park<sup>5</sup>, Tudor Luchian<sup>1</sup>

<sup>1</sup>Department of Physics, Alexandru I. Cuza University, 700506 Iasi, Romania

<sup>2</sup>Interdisciplinary Research Institute, Sciences Department, Alexandru I. Cuza University, 700506 Iasi, Romania

<sup>3</sup>Department of Chemistry, and Department of Physics and Astronomy, University of California, Irvine, CA 92617, USA

<sup>4</sup>Department of Bioinformatics, Kongju National University, Kongju, Republic of Korea, 32588

<sup>5</sup>Department of Biomedical Science and Research Center for Proteinaceous Materials (RCPM), Chosun University, Gwangju, Republic of Korea, 61452

## Materials and methods

**Reagents.** Potassium chloride (KCl), sodium chloride (NaCl), potassium hydroxide (KOH), hydrochloride acid (HCl) ultra-pure water (DNAase and RNAase free), MES (2-Morpholinoethanesulfonic acid monohydrate) and HEPES (N-(2-Hydroxyethyl)piperazine-N'-(2-ethanesulfonic acid) buffers, *n*-pentane HPLC-grade (10 mg/mL), hexadecane and wild-type  $\alpha$ -hemolysin ( $\alpha$ -HL) monomeric protein, were purchased from Sigma–Aldrich, Germany. The 1,2-diphytanoyl-sn-glycerophosphocholine (DPhPC) lipids were obtained from Avanti Polar Lipids, Alabaster, AL, USA.

**Sample preparation.** The dried form of ssDNAs samples were dissolved in 1 M NaCl solution in ultra-pure water buffered with TE (10 mM Tris, 1 mM EDTA) at pH = 8.2, and vigorously stirred using a Stuart BioCote vortex mixer (Sigma–Aldrich, Germany) at 1,400 rpm, for 3 min, in continuous mode. After solvation, the 100  $\mu$ M stock solutions of each sample were heated up to 95 °C for 20 min using an IKA Digital Block Heater (Cole-Parmer, USA) and slowly cooled down to 23 °C, to assure rehydration. All stock solutions were divided in aliquots and kept at – 20 °C.

**Nanopore electrophysiology.** The electrophysiology experiments were performed in a recording chamber consisting of two compartments denoted by *cis* (grounded) and *trans*, filed with different buffered used according to experimental protocol (i.e., 1 M KCl at pH 7, 5 or 4.5 and 4M KCl at pH = 4.5). The chambers were separated by a 25  $\mu$ m-thick Teflon film (Goodfellow, Malvern, MA, USA), containing an aperture of about 120  $\mu$ m in diameter, across on which the lipid bilayer was obtained after pre-treated the film with a mixture of 1:10 hexadecane in *n*-pentane. Addition of ~ 0.5 to 2  $\mu$ L  $\alpha$ -HL from a monomeric stock solution made in 0.5 M KCl to the grounded, *cis*-compartment, under ~ 10 min continuous stirring, led to insertion of a single heptameric  $\alpha$ -HL nanopore into the previously formed stable lipid membrane. Specific ssDNA sequences were

added at a 4  $\mu\text{M}$  bulk concentration on the *cis* side of the nanopore. By applying *trans* positive voltages ranging ( $\Delta V$ ) between +100 to +180 mV, with the help of a virtual instrument developed within LabVIEW 8.20 platform (National Instruments, USA) interfaced with an Axopatch 200B or Multiclamp 700B amplifier (Molecular Devices, USA), we recorded current fluctuations reflecting ssDNA interactions with a single  $\alpha$ -HL nanopore, in the voltage-clamp mode. The electrical signals were digitized at a sampling frequency of 50 kHz with a NI PCI 6221 16-bit acquisition board (National Instruments, USA) and low-pass filtered at 12 kHz. All the measurements were carried out on a vibration-free platform (BenchMate 2210, Warner Instruments, USA), shielded in a Faraday cage (Warner Instruments, USA), at a room temperature of  $\sim 23^\circ\text{C}$ . The numerical analysis of the ionic current blockades across the nanopore was performed within the statistics of exponentially distributed events using pClamp 6.03 (Axon Instruments, USA) and with a custom designed program in LabVIEW 2021 (National Instruments, USA), allowing us to manually select and automatically measure all properties of blockade events (amplitude, duration) and perform amplitude histograms analysis on selected traces spanning various time intervals. The non-linear fitting of translocation times across the  $\alpha$ -HL's lumen ( $\tau_{off-L}^-$ ) at distinct pH values was done in Mathematica 13.2 (Wolfram Research, USA) the graphic representations of data was done with the help of Origin 6 (Origin Lab, USA).

Table S1. The primary structures and corresponding molecular weights of the ssDNAs used herein

| <i>ssDNA</i> | <i>Sequence</i>              | $M_w$ (g/mol) |
|--------------|------------------------------|---------------|
| 22_ssDNA     | 5'-CCCCCCCATCACCGTATATCAC-3' | 6523          |
| 15_ssDNA     | 5'-GTGATATACGGTGAT-3'        | 4650          |
| 5_ssDNA      | 5'-AAAAA-3'                  | 1504          |

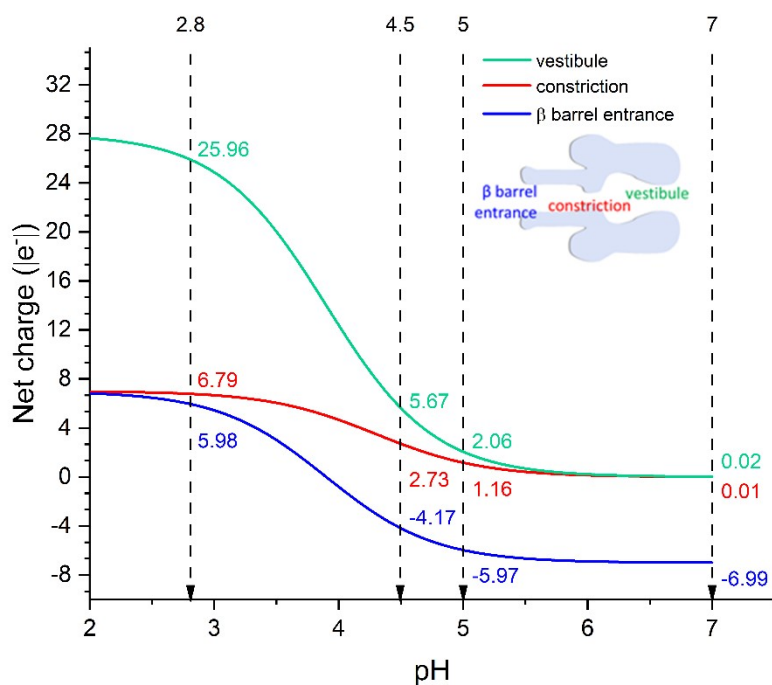


Figure S1. **pH alters significantly the electric charge distribution on the  $\alpha$ -HL nanopore.** By considering the pH-dependent ionizable residues within the vestibule (D13, D2, D4, D227, K8, R56, R104, K154), constriction (E111, K147) and  $\beta$ -barrel region (D127, D128, K131) contributed by each of the wild-type  $\alpha$ -HL's seven monomers, employing the Henderson–Hasselbalch equation, and considering the measured  $pK_a$  values of the aspartic acid (D) ( $pK_a = 3.9$ ) and glutamic acid (E) ( $pK_a = 4.3$ ) ionizable groups,<sup>1</sup> we estimated the net electric charge contributed by the vestibule, constriction region and  $\beta$ -barrel entrance of the wild-type  $\alpha$ -HL homo-heptamer in the range on acidic pH values. Vertical lines point to the selection of particular pH values used in our experiments.

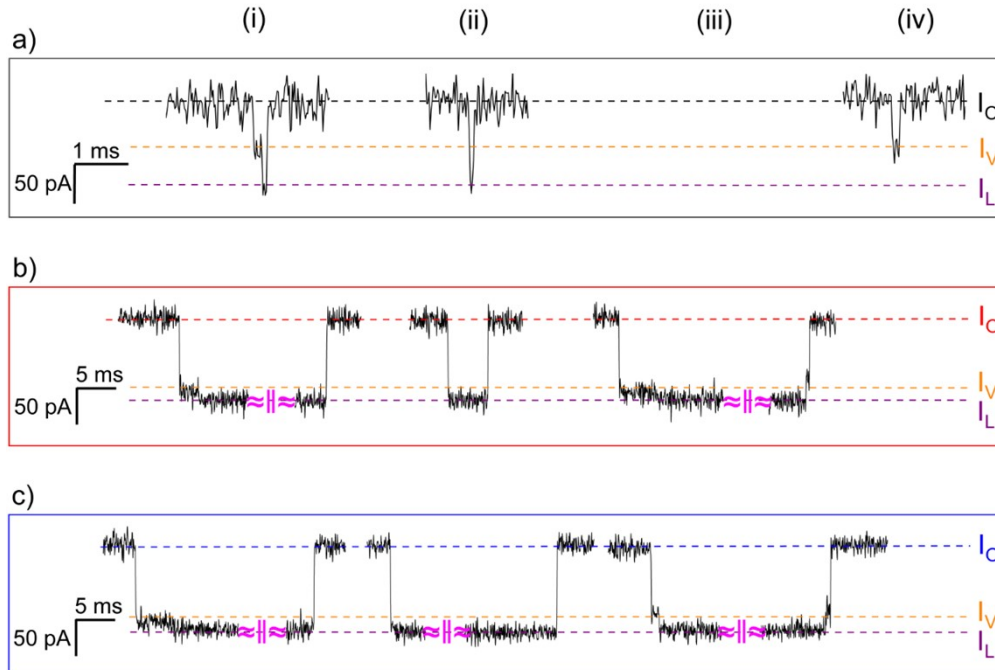


Figure S2. **Interaction of the 22\_ssDNA with the  $\alpha$ -HL nanopore.** Depending on the pH (panel a: pH = 7; panel b: pH = 5; panel c: pH = 4.5) various types of blockade events appear when 22\_ssDNA fragments are being electrophoretically funneled at the nanopore's vestibule entrance, in 1 M KCl and  $\Delta V = +140$  mV: (i) uni-directional passage of the analyte across the vestibule, and respectively lumen region of the protein, and release on the trans side ( $I_{O,cis} \rightarrow I_V \rightarrow I_L \rightarrow I_{O,trans}$ ); (ii) straight passage across the lumen and release on the trans side ( $I_{O,cis} \rightarrow I_L \rightarrow I_{O,trans}$ ); (iii) reversible passage of the analyte across the lumen, and release on the cis side without translocation ( $I_{O,cis} \rightarrow I_V \rightarrow I_L \rightarrow I_V \rightarrow I_{O,cis}$ ); (iv) reversible capture on the vestibule and release on the cis side, without entering the lumen ( $I_{O,cis} \leftrightarrow I_V$ ). Due to their length, the trace in b (i), b (iii) and (c), needed fracturing for better representation, as indicated by ( $\approx || \approx$ ).

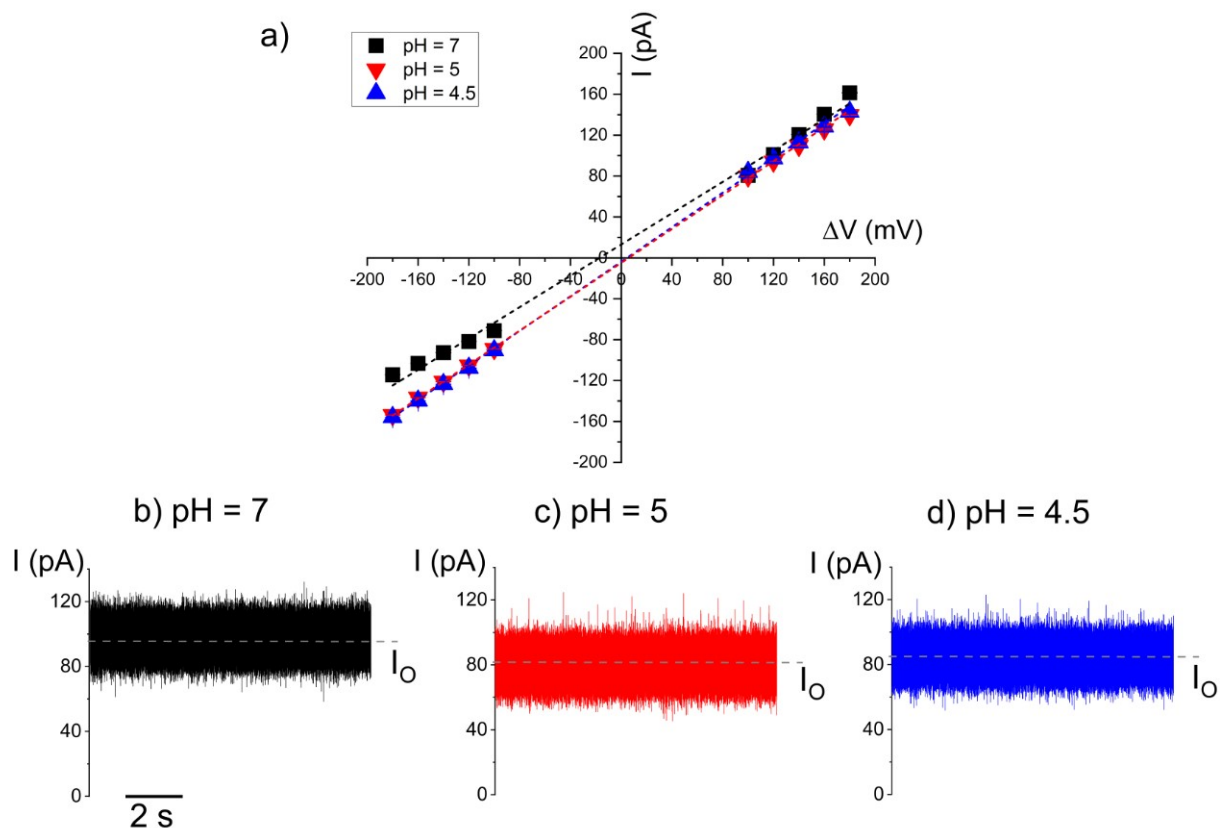
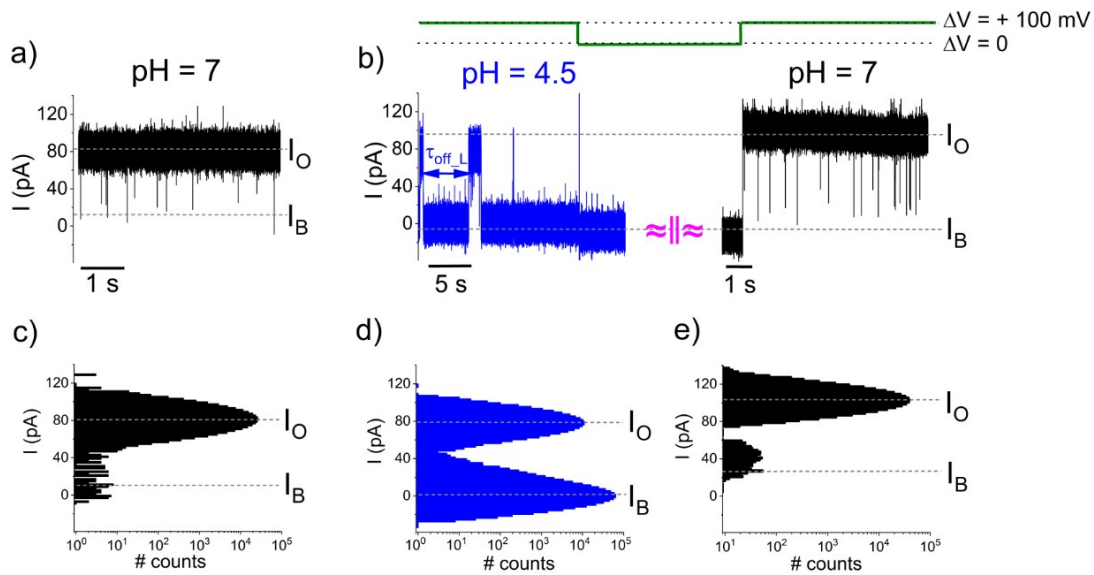


Figure S3. **The transport features of the  $\alpha$ -HL nanopore at various pH values.** (a)  $I$ - $\Delta V$  diagrams displaying the recorded ionic current through the open  $\alpha$ -HL nanopore at pH = 7, 5 and 4.5. (b-d) Representative traces excerpts showing the recorded ionic current through an open  $\alpha$ -HL nanopore at pH = 7, 5 and 4.5 respectively, revealing the absence of interfering gating events on the protein at a transmembrane potential of  $\Delta V = + 100$  mV.  $I_0$  denotes the open state of the nanopore. All experiments were carried out in an electrolyte containing 1 M KCl.



**Figure S4. The pH-induced lengthening of the cis-added 22\_ssDNA capture inside the  $\alpha$ -HL is reversible.** (a) With the cis-added 22\_ssDNA at a bulk concentration of 4  $\mu$ M, the analyte capture in the nanopore at pH = 7 and  $\Delta V = + 100$  mV is seen as fast, reversible changes in the ionic current from the open state ( $I_O$ ) to blocked state ( $I_B$ ), whereby a single 22\_ssDNA molecule resides temporarily inside the nanopore. (b) A subsequent change in the electrolyte acidity to pH = 4.5 triggers a dramatic lengthening of times spent by the analyte inside the  $\alpha$ -HL's lumen ( $\tau_{off-L}^- = 9.3 \pm 1.02$  seconds (average  $\pm$  S.E.M.)), whereas changes within the same experiment of the electrolyte acidity, with controlled drops of KOH back to pH = 7, determines the recovery of times spent by the analyte inside the  $\alpha$ -HL's lumen back to values measured initially in neutral electrolytes ( $\tau_{off-L}^- = 1.6E-4 \pm 0.01E-4$  seconds (average  $\pm$  S.E.M.)). In panel (c) we represent the amplitude histograms of the blockade events seen initially, when a single 22\_ssDNA molecule resides temporarily inside the nanopore at pH = 7, of those measured when the pH was changed to 4.5 (d), and upon re-setting the acidity back to pH = 7 (e).

## **Brief account on the distribution of 22\_ssDNA translocation times across the $\alpha$ -HL's lumen within the first-passage-time theory**

To simplify the problem, we assumed for the lumen captured ssDNA fragments a kinetics resembling free translocation, and included ssDNA–nanopore interactions lumped into the effective value of the diffusion coefficient. As a particular element of complexity, the electro-osmotic flow generated across the positively biased, anionic  $\alpha$ -HL nanopore runs on the same direction of the ssDNA electrophoresis. For simplicity, we chose to lump the effect of the electro-osmotic flow in the measured, effective diffusion constant.

As described in literature,<sup>2,3</sup> we modeled the sojourn time of single 22\_ssDNA inside the  $\alpha$ -HL's  $\beta$ -barrel as the first passage time for one-dimensional diffusion of a charged molecules in a constant electric field, with the analyte in a linear conformation along its moving direction. In other words, we assume a reduced probability of detecting fragments in a folded configuration while traversing the  $\beta$ -barrel section of the nanopore. We take into account that the potential drop across the  $\alpha$ -HL's vestibule is small, and during the analyte passage through the  $\beta$ -barrel of length

$l_{\text{lumen}}$ , only a fraction of the 22\_ssDNA molecule  $\left(\frac{l_{\text{lumen}}}{L_c}\right)$  ( $L_c$  represent the contour length of the 22\_ssDNA fragment) feels the electric field inside the lumen.<sup>2</sup> We also considered that the transport of the  $\beta$ -barrel captured 22\_ssDNA fragment is controlled essentially by the applied transmembrane voltage ( $\Delta V$ ), as well as electrostatic interactions with various regions from the nanopore's inner surface. Although disputable, we neglect entropic changes suggestive of conformational changes of the captured molecule (e.g., ssDNA (un)coiling inside the nanopore), as main contributors to the free energy profile.



In this over-simplified scenario, the probability density function ( $F_1(t)$ ) of the sojourn times of the 22\_ssDNA inside the  $\beta$ -barrel lumen is given by:

$$F_1(t) = \frac{d}{\sqrt{4\pi Dt^3}} e^{-\frac{(d-vt)^2}{4Dt}} \quad (1)$$

where D and v are the diffusion coefficient and the drift velocity of the segment of the 22\_ssDNA inside the nanopore, respectively.

As the contour length ( $L_c$ ) for the 22 bases ssDNA ( $\sim 13.2$  nm) is longer than the lumen ( $l_{lumen} \sim 5$  nm), we replaced  $d = L_c + l_{lumen}$ .<sup>2</sup> It then follows that average value of the times ( $\tau_{off\_L}^-$ ) describing full translocation events of single 22\_ssDNA across the  $\beta$ -barrel lumen writes:

$$\tau_{off\_L}^- = \int_0^{\infty} \tau_{off\_L} F_1(t) dt = \frac{L_c + l_{lumen}}{v} \quad (2)$$

By the virtue of arguments presented above, v coincides with the electrophoretic velocity ( $v_{electrophoretic}$ ) of the 22\_ssDNA molecule and its modulus writes as:

$$v_{electrophoretic} = \mu E = \mu \frac{\Delta V}{l_{lumen}} \quad (3)$$

where  $\Delta V$  is the applied transmembrane potential,  $\mu$  represents the electrophoretic mobility of the

22\_ssDNA within the lumen and  $E = \frac{\Delta V}{l_{lumen}}$  represents the modulus of the electric field intensity sensed during passage.

Thus:

$$\tau_{off-L}^- = \frac{L_c + l_{lumen}}{\frac{\Delta V}{\mu \frac{l_{lumen}}{L_c}}} \quad (4)$$

By combining this with the electrophoretic mobility ( $\mu$ ) obtained from the Einstein relation:

$$\mu = \frac{|Z_{eff}| |e^-| D \left( \frac{l_{lumen}}{L_c} \right)}{k_B T} \quad (5)$$

where  $Z_{eff}$  represents the effective valence of the 22\_ssDNA,  $e^-$  is the electron charge,  $D$  the diffusion coefficient of the 22\_ssDNA inside the nanopore, and by applying the correction on the electric mobility of the ssDNA across the  $\beta$ -barrel lumen, to account for the fact that only a fraction

$\left( \frac{l_{lumen}}{L_c} \right)$  from the 22\_ssDNA fragment moves in the electric field inside the lumen, we then obtain a theoretical relation  $\tau_{off-L}^-$  vs.  $\Delta V$ .

In our estimations, we used for the electrical charge a value of  $-0.3 |e^-|$  per base in 1 M KCl,<sup>2,4</sup> thus arriving at  $Z_{eff} = -6.6$  for the 22\_ssDNA fragment at neutral pH. Note however, that with lowering the electrolyte pH, adenine ( $pK_a$  of the N1 atom  $\sim 4.25$ ) and respectively cytosine ( $pK_a$  of the N3 atom  $\sim 4.6$ ) bases can accept protons, thus becoming positively charged and leading to a reduction in the effective negative charge of the ssDNA molecule. By employing the Henderson–Hasselbalch equation and replacing the corresponding  $pK_a$  values for adenine and cytosine (vide supra), it follows that at pH = 4.5, the 12 cytosines on the 22\_ssDNA fragment generate a net charge of  $+6.7 |e^-|$  whereas the 5 adenines generate a net charge of  $+1.8 |e^-|$ . To a first approximation and for consistency, one may consider that similar physical mechanisms that lead to the 70 % charge reduction extent per phosphate group in 1 M KCl (vide supra), e.g.

charge condensation, also reduce the positive charge brought about by the protonated adenine and cytosine bases, thus bringing the overall effective positive charge on the 22\_ssDNA at pH = 4.5, to  $+2.55 |e^-|$ . This positive charge adds up to the negative charge on the ssDNA fragments, so in a rough approximation, the  $Z_{\text{eff}}$  for a 22\_ssDNA fragment bathed at pH = 4.5, decreases to -4.05.

On the next step, we recorded the kinetic behavior of the 22\_ssDNA while interacting with the  $\alpha$ -HL at the pH = 7 and pH = 4.5, to obtain experimental data pertaining to the  $\tau_{\text{off}_L}^-$  vs.  $\Delta V$  dependence. For brevity, in Figure S5 we present original, representative traces recorded at applied transmembrane potentials of  $\Delta V = +120$  mV and +160 mV, along with the corresponding events diagram as well as the experimentally derived  $\tau_{\text{off}_L}^-$  vs.  $\Delta V$  dependence.

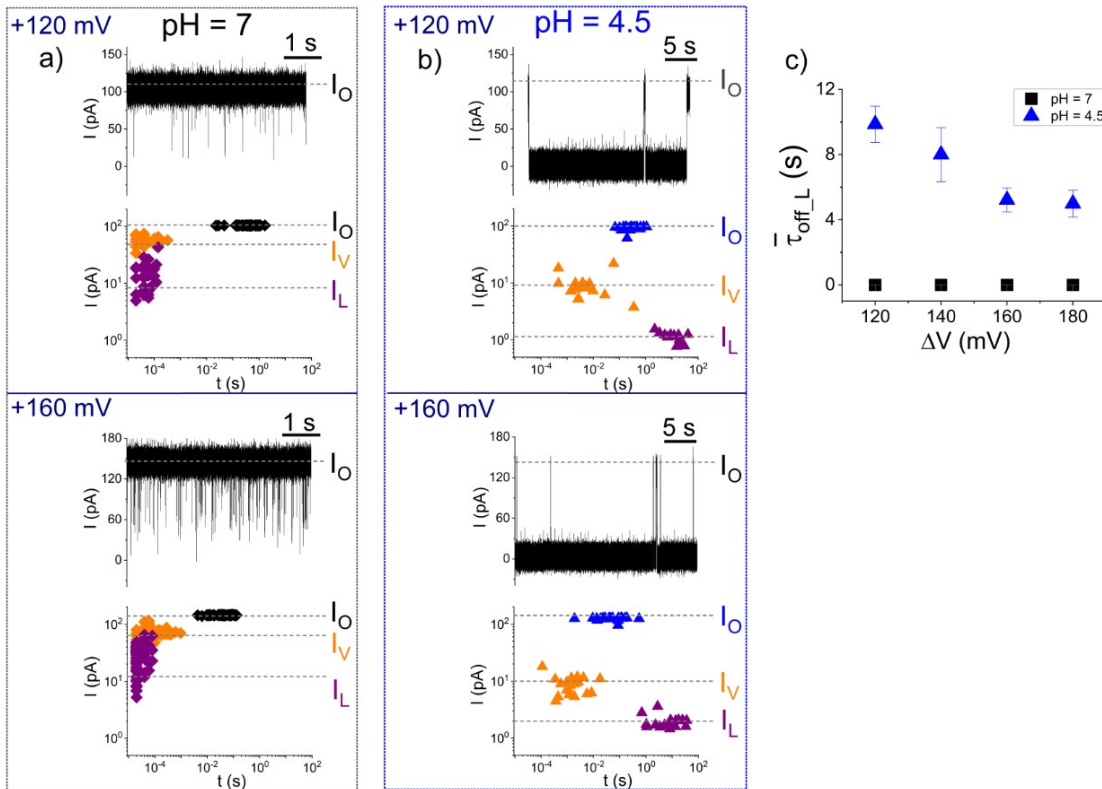


Figure S5. **The applied transmembrane voltage alters the pH-dependent 22\_ssDNA- $\alpha$ -HL interactions.** Representative electrophysiology traces and the two-dimensional scatter distributions of blockade durations corresponding to the blockade substates seen during 22\_ssDNA translocation, i.e.  $I_O$  (open nanopore),  $I_V$  (22\_ssDNA lodged inside the  $\alpha$ -HL's vestibule) and  $I_L$  (22\_ssDNA lodged inside the  $\alpha$ -HL's lumen) recorded at  $\Delta V = +120$  mV and  $\Delta V = +160$  mV in an electrolyte containing 1 M KCl buffered at pH = 7 (a) and respectively pH = 4.5 (b). The bulk concentration of the cis-added 22\_ssDNA was 4  $\mu$ M. (c) The voltage dependence of the 22\_ssDNA translocation times across the  $\alpha$ -HL's lumen ( $\tau_{off-L}^-$ ) at distinct pH values.

By replacing known values for the remaining terms in expressions 4 and 5 ( $T=296$  K,  $l_{lumen} = 5 \times 10^{-9}$  m,  $L_c = 13 \times 10^{-9}$  m), and by non-linear fitting of data shown in Figure S5, c with the function given by Eq. (4), we arrived at  $D = 2.4 \times 10^{-13} m^2 s^{-1}$  at pH = 7 and respectively  $D = 1.58 \times 10^{-18} m^2 s^{-1}$  at pH = 4.5 (Figure S6).

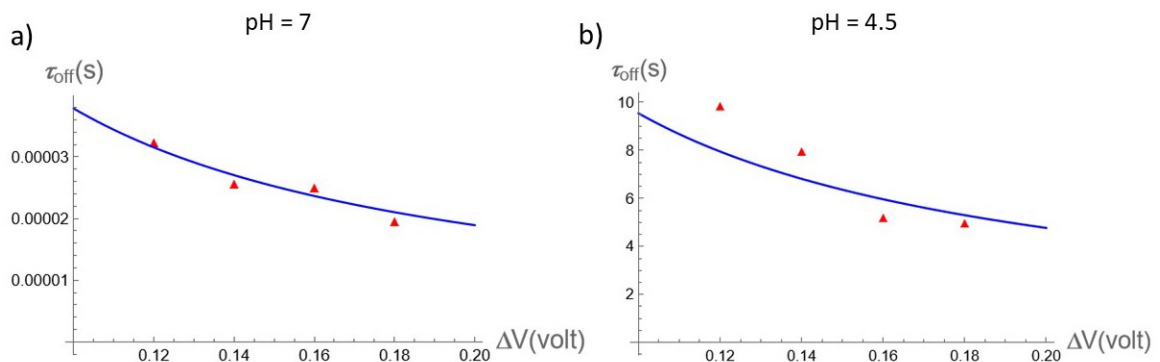


Figure S6. **Experimental determination of 22\_ssDNA diffusion coefficient inside the nanopore.** The non-linear fit of experimental data collected at pH = 7 (a) and respectively pH = 4.5 (b) with the theoretically derived  $\tau_{off-L}^-$  vs.  $\Delta V$  dependence (see text) allowed the determination of diffusion coefficient values of the lumen-translocation 22\_ssDNA in both cases.

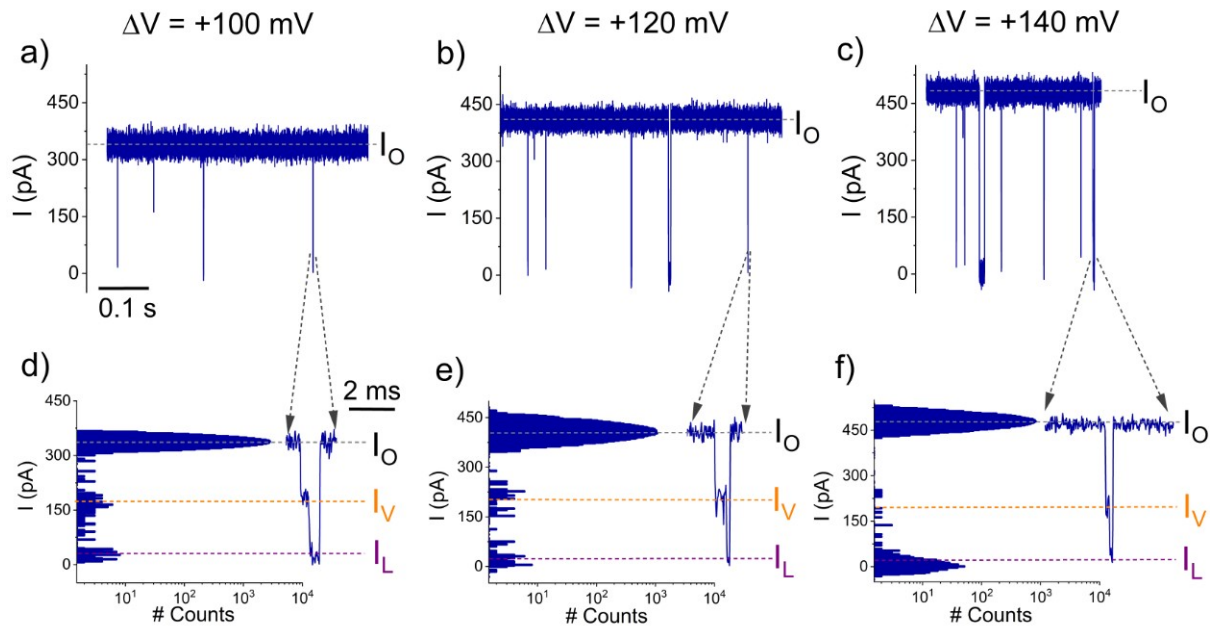


Figure S7. **In high ionic strength, the low-pH induced slowdown of 22\_ssDNA across the nanopore ceases.** Selected experimental traces showing the 22\_ssDNA –  $\alpha$ -HL interactions recorded at  $\Delta V = +100$  mV (a),  $\Delta V = +120$  mV (b) and  $\Delta V = +140$  mV (c), in an electrolyte containing 4 M KCl buffered at pH = 4.5. The bulk concentration of the cis-added 22\_ssDNA was 4  $\mu$ M. In the corresponding zoomed-in panels we display the distinct conductive substates ( $I_O$ ,  $I_V$ ,  $I_L$ ) seen during analyte translocation and the amplitude histogram of blockade events recorded at  $\Delta V = +100$  mV (d),  $\Delta V = +120$  mV (e) and  $\Delta V = +140$  mV (f). The statistical analysis on the

blockade durations across the lumen and vestibule recorded at  $\Delta V = +140$  mV revealed average values of  $\tau_{off,L}^- = 0.71E-4 \pm 0.08E-4$  seconds (average  $\pm$  S.E.M.) and respectively  $\tau_{off,V;pH=4.5}^- = 1.12E-4 \pm 0.2E-4$  seconds (average  $\pm$  S.E.M.), and the amplitude histogram of blockade events resulted in the relative blockade values induced by the 22\_ssDNA fragments while translocating the lumen ( $\frac{\Delta I_L}{I_0} = -0.94 \pm 0.007$ ) and respectively the vestibule ( $\frac{\Delta I_V}{I_0} = -0.51 \pm 0.01$ ).

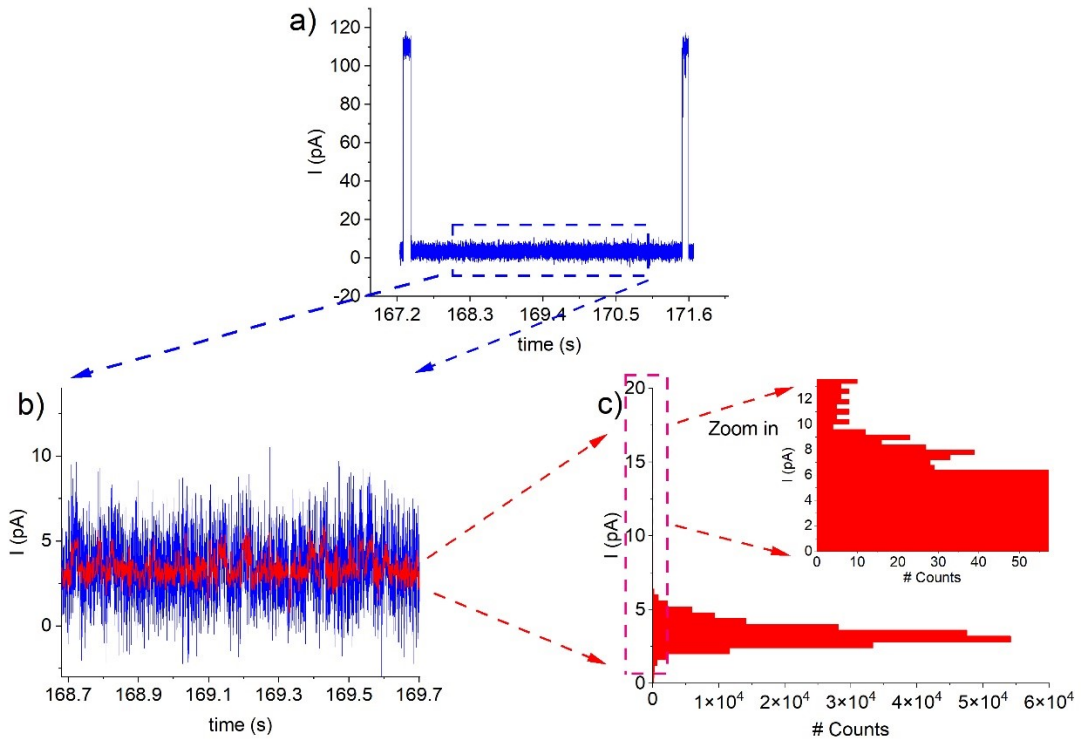


Figure S8. **The low-pH induced slowdown of 22\_ssDNA across the nanopore permits visualization of blockade events associated with analyte translocation.** (a) Selected experimental trace showing the 22\_ssDNA –  $\alpha$ -HL interactions recorded at  $\Delta V = +140$  mV in an

electrolyte containing 1 M KCl buffered at pH = 5, with the analyte added on the cis side of the membrane. (b) The low-pass filtering ( $f_c = 300$  Hz) of the data segment delimited by the blue, dashed rectangle in (a), associated with the occupancy of the nanopore by a single 22\_ssDNA molecule, reveals reversible blockades associated with the uni-directional movement of the captured 22\_ssDNA molecule across the nanopore (red trace). (c) Amplitude histogram of the filtered record shown in (b), displaying the discrete amplitude values of the current fluctuations accompanying 22\_ssDNA movement across the nanopore, also seen in the zoomed in inset.

## References

- (1) Grimsley, G. R.; Scholtz, J. M.; Pace, C. N. A Summary of the Measured pK Values of the Ionizable Groups in Folded Proteins. *Protein Sci.* **2009**, *18* (1), 247—251. DOI: 10.1002/pro.19
- (2) Li, J., Talaga, D. S. The Distribution of DNA Translocation Times in Solid-State Nanopores, *J. Phys. Condens. Matter* **2010**, *22* (45), 454129. DOI: 10.1088/0953-8984/22/45/454129
- (3) Ling, D. Y.; Ling, X. S. On the Distribution of DNA Translocation Times in Solid-State Nanopores: An Analysis Using Schrödinger's First-Passage-Time Theory. *J. Phys.: Condens. Matter* **2013**, *25* (37), 375102. DOI: 10.1088/0953-8984/25/37/375102
- (4) Smeets, R. M.; Keyser, U. F.; Krapf, D.; Wu, M. Y.; Dekker, N. H.; Dekker, C. Salt Dependence of Ion Transport and DNA Translocation through Solid-State Nanopores. *Nano Lett.* **2006**, *6* (1), 89–95. DOI: 10.1021/nl052107w